Relaxation and Hysteresis in a Periodically Forced Swift-Hohenberg System

AUTHOR(S):

Morino, Kai; Ouchi, Katsuya; Miyazaki, Syuji

Progress of Theoretical Physics, Vol. 125, No. 6, June 2011

Relaxation and Hysteresis in a Periodically Forced Swift-Hohenberg System

Kai MORINO,[1,*)] Katsuya OUCHI[2] and Syuji MIYAZAKI[1]

[1]*Department of Applied Analysis and Complex Dynamical Systems, Graduate School of Informatics, Kyoto University, Kyoto 606-8501, Japan*
[2]*Kobe Design University, Kobe 651-2196, Japan*

(Received April 2, 2010; Revised March 18, 2011)

The relaxation and hysteresis of a periodically forced Swift-Hohenberg (SH) equation as a phenomenological model for the magnetic domains of a garnet thin film in an oscillating magnetic field are studied. It is already known that the unforced SH equation settles down to a single type of spatial structure called a stripe pattern, and that the relaxation process yields a scaling law for the structure factor. Two types of temporally oscillating spatial structure consisting of stripe and polka-dot patterns have also been asymptotically observed in the case of a periodically forced SH equation. Relaxation scaling behaviors are studied for these two patterns. It is also shown for the forced case that a hysteresis is observed in the vicinity of the boundary between two different spatial patterns in the phase diagram.

Subject Index: 051

§1. Introduction

Many studies have been compiled on pattern dynamics far from equilibrium such as thermal convection, chemical reactions and biological pattern formation.[1)–3)] One of the example of such phenomena is the onset of Rayleigh-Benard convection and the formation of roll patterns. It is well known that the thermal convection is modeled by the Swift-Hohenberg (SH) equation.[4)–6)] This equation is derived by considering the Navier-Stokes equation in the Boussinesq approximation and the thermal diffusion equation, the boundary conditions of which are given by two infinite horizontal plates with temperatures T_0 and $T_0 + \Delta T$. When the Rayleigh number R, which is a dimensionless temperature difference ΔT, is larger than a critical value R_c, convection rolls emerge. The linearized equations give two stable eigenvalues corresponding to two horizontal directions in the velocity field and two unstable ones corresponding to the vertical direction and another direction in the temperature field. Neglecting the stable modes and only considering the wavelengths near the most unstable wavelength k_0, which can be set to unity without loss of generality, we have the SH equation

$$\frac{\partial s(\boldsymbol{r},t)}{\partial t} = \left[\epsilon - (\nabla^2 + k_0^2)^2\right] s(\boldsymbol{r},t) - \{s(\boldsymbol{r},t)\}^3, \tag{1·1}$$

where $s(\boldsymbol{r},t)$ is a scalar state variable as a function of two-dimensional position $\boldsymbol{r}$ and time t, and ϵ is a control parameter that is proportional to the distance from the

*) Present address: Department of Mathematical Informatics, Graduate School of Information Science and Technology, University of Tokyo, Tokyo 113-8656, Japan.

critical point $R - R_c$. When ϵ is negative, the values of $s(\boldsymbol{r}, t)$ for $t \to \infty$ uniformly vanish, which represents thermal conductance without convection. When ϵ is positive, the asymptotic spatial structure of $s(\boldsymbol{r}, t)$ is characterized by a stripe pattern, which represents convection rolls. A generalized SH equation was also proposed, which shows pattern dynamics different from the original ones.[7)]

Let $\tilde{S}(\boldsymbol{k}, t)$ be the intensity of the Fourier transform of $s(\boldsymbol{r}, t)$, defined by $\tilde{S}(\boldsymbol{k}, t) \equiv |\int s(\boldsymbol{r}, t) \exp(i\boldsymbol{k} \cdot \boldsymbol{r})\, d\boldsymbol{r}|^2$, where $\boldsymbol{k}$ is a two-dimensional wave vector. The amplitude k and angle θ are given by $\boldsymbol{k} = (k\cos\theta, k\sin\theta)$ as cylindrical coordinates. Because $\tilde{S}(\boldsymbol{k}, t)$ does not depend strongly on the angle θ but strongly on the amplitude k owing to the isotropy of the system, we introduce $S(k, t)$, which is referred to as the structure factor in the following, by averaging $\tilde{S}(\boldsymbol{k}, t)$ over the angle direction as $S(k, t) = \frac{2}{\pi} \int_0^{\pi/2} \tilde{S}(k, \theta, t) d\theta$, which has a sharp peak at approximately k_0.

Not only in a convective system but also in a uniaxial ferromagnetic garnet thin film, various spatial patterns are observed. The films without an external field have labyrinthine magnetic domain structures. Upon adding a temporally oscillating magnetic field perpendicular to the film, the domain structure changes to various patterns, depending on the amplitude and frequency of the applied field.[8),9)] Noting that garnet films have the magnetic easy axis perpendicular to the film plane, we use a two-dimensional continuous Ising spin system in order to describe the domain structures. Noting that when no magnetic field is applied, the system has a spin-flip symmetry and the domain structure is labyrinthine, Tsukamoto et al. considered the pattern dynamics of the following periodically forced SH equation:[10)]

$$\frac{\partial s(\boldsymbol{r}, t)}{\partial t} = \left[\epsilon - (\nabla^2 + k_0^2)^2\right] s(\boldsymbol{r}, t) - \{s(\boldsymbol{r}, t)\}^3 + h\sin(\Omega t). \tag{1·2}$$

They found that a stripe pattern, a polka-dot pattern and a spatially uniform state with temporal oscillation are observed, depending on the values of the amplitude h and angular frequency Ω of the external field.[10)] The phase diagram of the spatial pattern in the Ω-h plane is shown in Fig. 1. It should be noted that Tsukamoto et al.[10)] classified the patterns in more detail. However, we confine ourselves to the above three patterns.

We assume the following scaling law for the structure factor:

$$S(k, t) = t^{\alpha} f_{h,\Omega}\big((k_0 - k)t^{\alpha}\big), \tag{1·3}$$

introduced by Elder et al., who estimated the scaling exponent as $\alpha = 1/5$ for the original SH equation and $\alpha = 1/4$ for the SH equation with additional noise in the case of $\epsilon = 0.25$.[11),12)] Hou et al. found logarithmic behavior, $S(k_0, t) \propto \log t$, for $\epsilon = 0.75$ at zero noise.[13)] Note that the scaling function in our case is not universal and depends on the amplitude h and angular frequency Ω of the external field.

In this paper, we study relaxation and hysteresis in the case of a periodically forced SH equation. In §2, we study scaling behaviors for the stripe and polka-dot patterns and compare them with the results for the unforced case. The bistability of the stripe and polka-dot patterns is discussed in §3. The final section is devoted to concluding remarks.

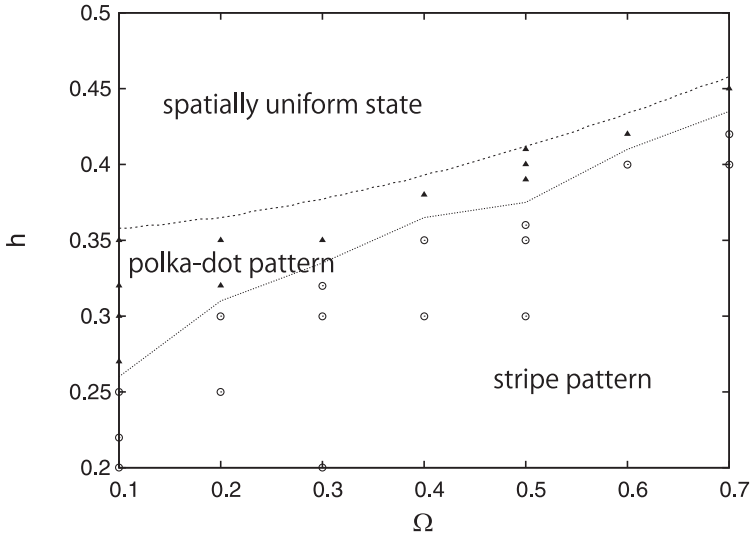

Fig. 1. Phase diagram of the spatial patterns of $s(\boldsymbol{r}, t)$ in Ω-h space. The symbols ○ and ▲ represent the stripe pattern and polka-dot pattern, respectively. A spatially uniform state is stable above the dashed line. No clear boundary exists between the stripe and polka-dot patterns. Around the dotted line, both patterns coexist.

§2. Scaling related to relaxation phenomena in a periodically forced Swift-Hohenberg system

In the stripe and polka-dot regions of the phase diagram (Fig. 1), we integrate Eq. (1·2) numerically using the Euler difference scheme adopted in the paper of Elder et al.,[11] in which the discretized Laplacian includes contributions from the nearest and second-nearest neighbors. We also calculate the time evolution of the structure factor $S(k, t)$. Other parameters are set as follows: $k_0 = 1$, $\epsilon = 0.25$, $\Delta x = \Delta y = \pi/4$, $\Delta t = 0.01$ and 512×512 system size, unless stated otherwise. We prepare 196 different sets of initial conditions as an ensemble, and the ensemble average is used to obtain our results.

The time dependence of the half width of $S(k, t)$ for $h = 0.3$ and $\Omega = 0.5$, yielding a stripe pattern, is plotted with the symbols ($\times$) in Fig. 2(a) and compared with the result for the unforced case ($+$). The half width is found to decrease in proportion to $t^{-1/5}$. We also confirm that the maximum value of $S(k, t)$ diverges in proportion to $t^{1/5}$. Hence, the scaling exponent α in Eq. (1·3) is estimated for a stripe pattern to be $\alpha = 1/5$, which coincides with that for the original unforced SH equation. The scaling law (1·3) is also numerically confirmed to have the scaling exponent $\alpha = 1/5$ as shown in Fig. 2(b).

The time dependence of the half width of $S(k, t)$ for $h = 0.4$ and $\Omega = 0.5$, yielding a polka-dot pattern, is plotted with the symbols ($\times$) for system size 256×256, ($*$) for 512×512 and ($\square$) for 1024×1024 in Fig. 3 and compared with the result for the unforced case ($+$). The half width is found not to decrease simply in proportion to $t^{-\alpha}$.

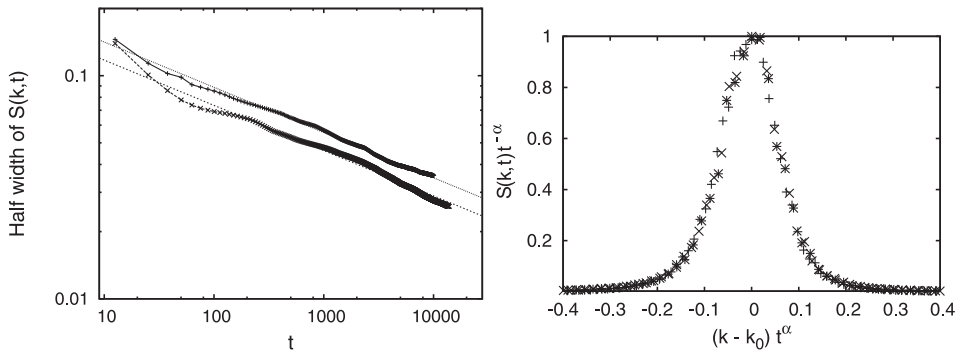

(a) (b)

Fig. 2. $(h, \Omega) = (0.3, 0.5)$, yielding a stripe pattern with the scaling exponent $\alpha = 1/5$. (a) Half width of $S(k,t)$ plotted against time t. The symbols $+$ and $\times$ represent the unforced case $(h = 0)$ and the periodically forced case, respectively. (b) $S(k,t)t^{-\alpha}$ plotted against $(k - k_0)t^{\alpha}$. The symbols $+$, $\times$ and $*$ correspond to $t = 1004.8$, 3768.0 and 6280.0, respectively. The values of the ordinate are normalized so that the maximum is equal to unity.

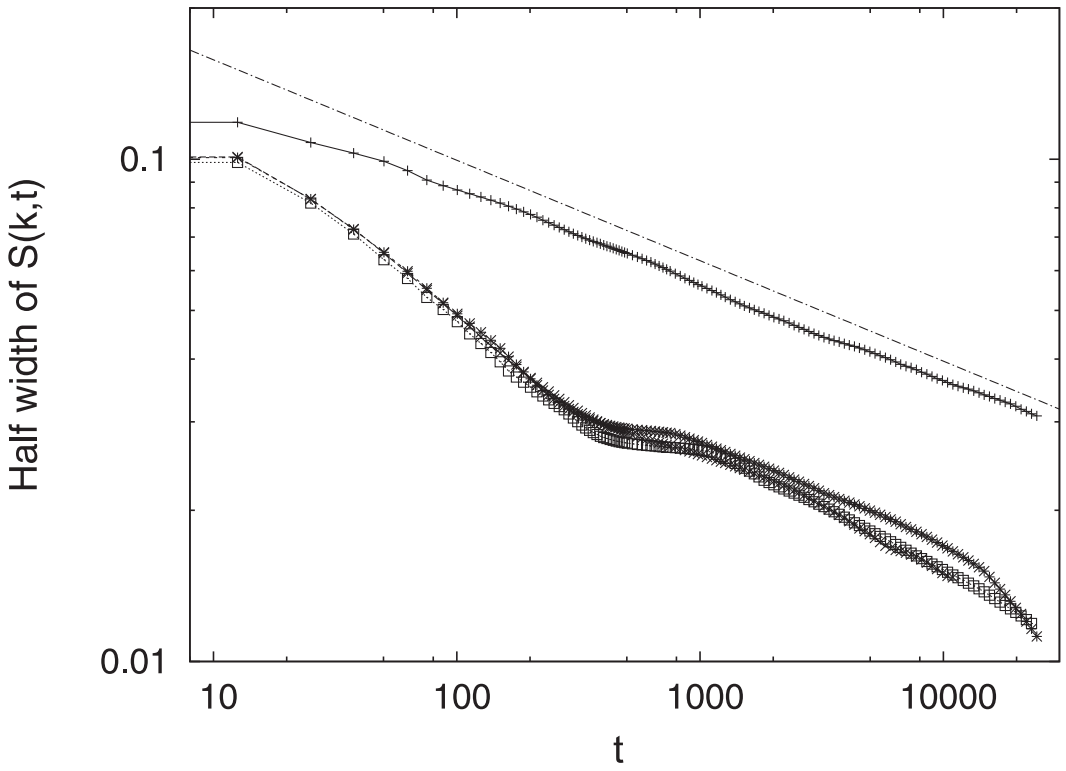

Fig. 3. Time dependence of the half width of $S(k,t)$ for $h = 0.4$ and $\Omega = 0.5$, yielding a polka-dot pattern, plotted with the symbols $(\times)$ for system size 256×256, $(*)$ for 512×512 and $(\square)$ for 1024×1024, compared with the result for the unforced case $(+)$.

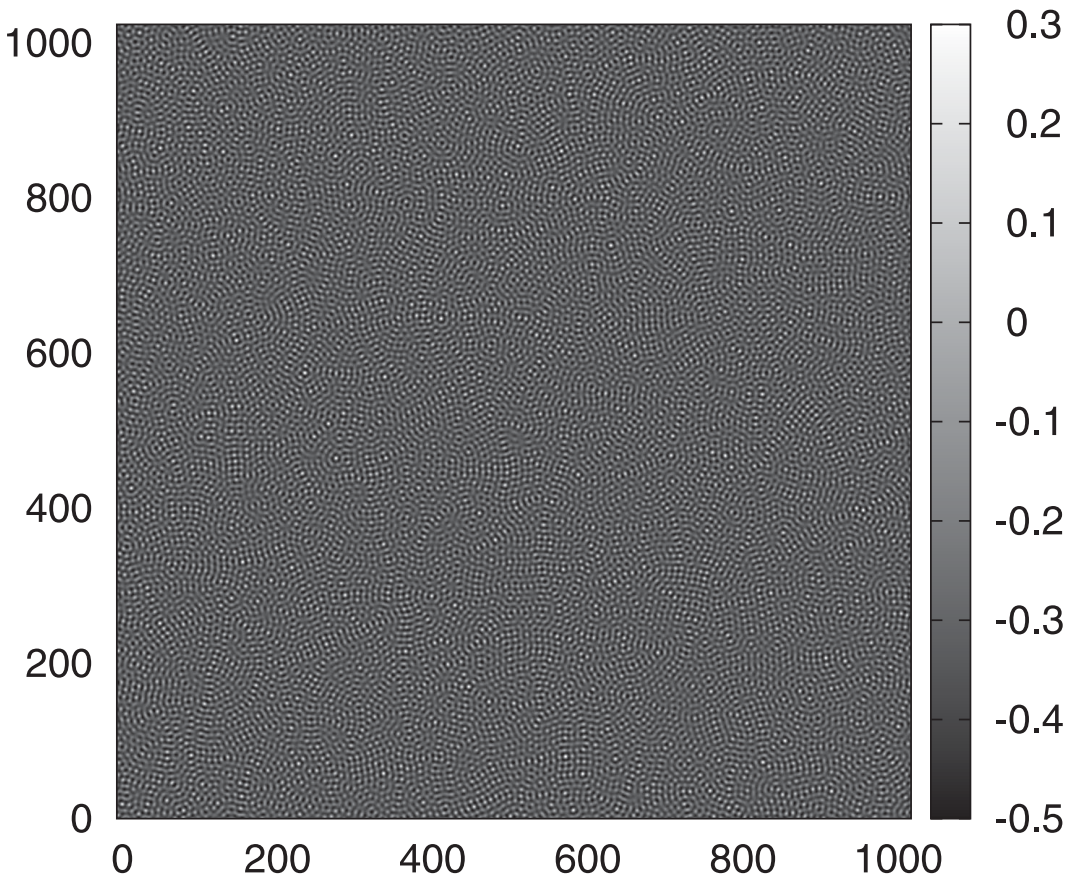

Fig. 4. Irregular pattern for $h = 0.4$ and $\Omega = 0.5$ at $t = 126$.

Three stages of relaxation exist. In the initial stage, $t \lesssim 500$, a very irregular pattern is observed as shown in Fig. 4. In the middle stage, $500 \lesssim t \lesssim 1000$, a patchwork structure appears. A regular polka-dot pattern is found in a single patch. The size of the patch is widely distributed, and the average size of the patch is much smaller than the system size. The square lattice on which a polka-dot pattern in a specific patch exists is directed randomly, as shown in Fig. 5. In the final stage, $t \gtrsim 1000$, the average size of the patch is comparable with the system size, as shown in Fig. 6. At this stage, there is a marked finite-size effect. The scaling behavior described by Eq. (1·3) is thought to hold in the middle stage. However, the scaling region $500 \lesssim t \lesssim 1000$ is too narrow in our case to numerically confirm Eq. (1·3).

§3. Bistability of two patterns near the boundary in the phase diagram

First we set $(h, \Omega) = (0.375, 0.5)$, which is located in the boundary region between the stripe and polka-dot patterns in the phase diagram shown in Fig. 1. Two different sets of random initial conditions $s(\boldsymbol{r}, 0)$ yield two different asymptotic spatial patchwork-like patterns with temporal oscillation consisting of a stripe part and

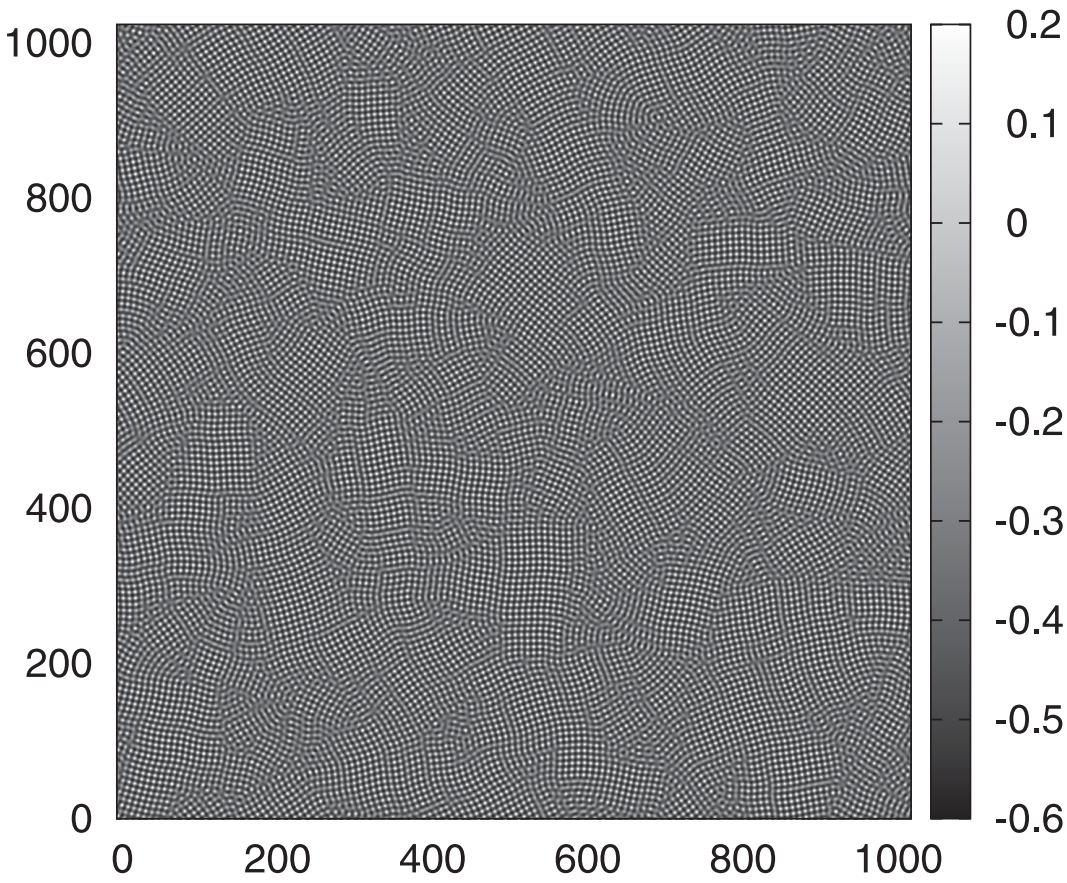

Fig. 5. Patchwork pattern for $h = 0.4$ and $\Omega = 0.5$ at $t = 628$. In a single patch, a regular polka-dot pattern is observed. The average patch size is much smaller than the system size.

a polka-dot part, as shown in Fig. 7.

A set of initial conditions $s(\boldsymbol{r}, 0)$ for $(h, \Omega) = (0.375, 0.5)$ is generated as an asymptotic numerical solution $s(\boldsymbol{r}, \tau)$ for $(h, \Omega) = (0.35, 0.5)$ with large τ, yielding a global stripe pattern, which leads to a global stripe pattern $s(\boldsymbol{r}, t)$ for $(h, \Omega) = (0.375, 0.5)$, as shown in Fig. 8(a). Another set of initial conditions $s(\boldsymbol{r}, 0)$ for $(h, \Omega) = (0.375, 0.5)$ is generated as an asymptotic numerical solution $s(\boldsymbol{r}, \tau)$ for $(h, \Omega) = (0.41, 0.5)$ with large τ, yielding a global polka-dot pattern, which leads to a global polka-dot pattern $s(\boldsymbol{r}, t)$ for $(h, \Omega) = (0.375, 0.5)$, as shown in Fig. 8(b).

We fix the frequency of the external field as $\Omega = 0.5$ in the following. A set of initial conditions $s(\boldsymbol{r}, 0)$ generated as an asymptotic numerical solution $s(\boldsymbol{r}, \tau)$ with large τ for a smaller value of h, yielding a global stripe pattern, leads to a global stripe pattern $s(\boldsymbol{r}, t)$ in the range $0.35 \leq h \leq 0.385$, which is plotted in Fig. 9 with the symbol ($\circ$) connected by the lower solid line. For $h > 0.385$, the above set of initial conditions is unstable and settles down to a global polka-dot pattern, which is plotted with the symbol ($\bullet$). In the same way, a set of initial conditions $s(\boldsymbol{r}, 0)$ generated as an asymptotic numerical solution $s(\boldsymbol{r}, \tau)$ with large τ for a larger value

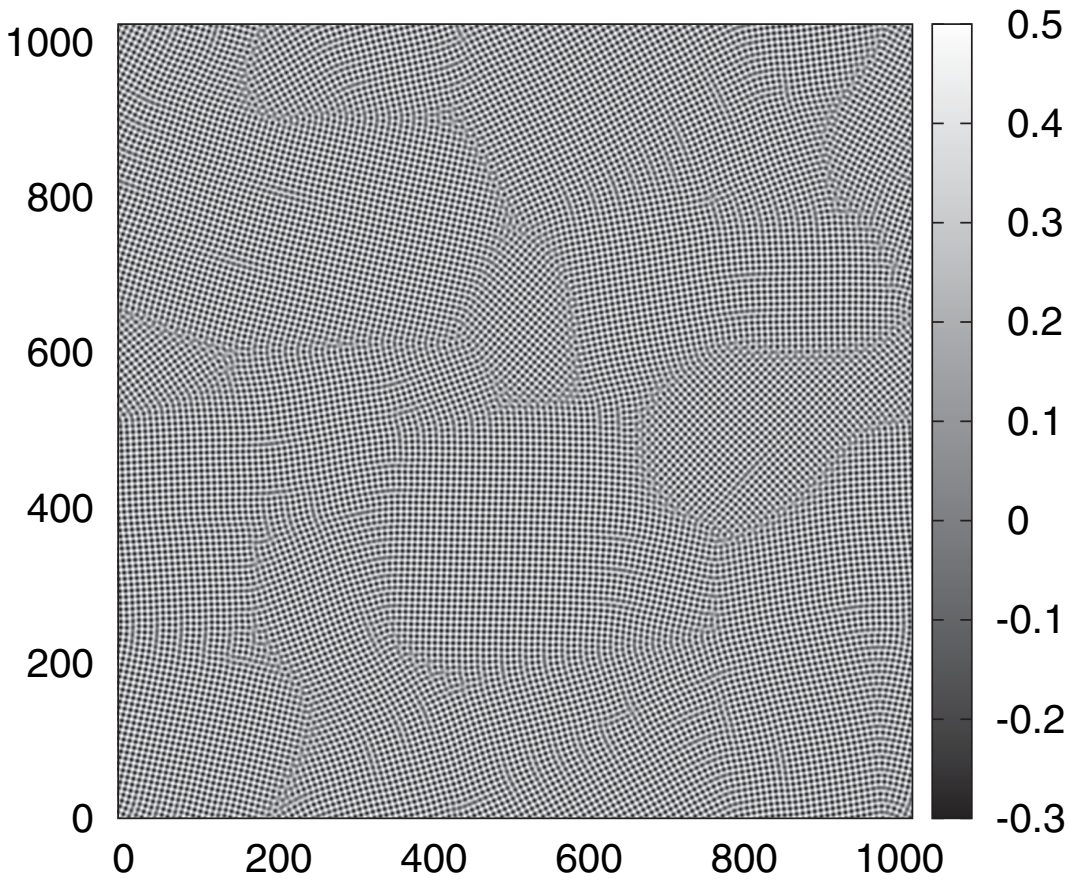

Fig. 6. Patchwork pattern for $h = 0.4$ and $\Omega = 0.5$ at $t = 12560$. The average patch size is comparable with the system size.

of h, yielding a global polka-dot pattern, leads to a global polka-dot pattern $s(\boldsymbol{r}, t)$ in the range $0.371 \leq h \leq 0.41$, which is plotted with the symbol (△) connected by the upper solid line. For $h < 0.371$, the above set of initial conditions is unstable and settles down to a global stripe pattern, which is plotted with the symbol (▲). We observe a hysteresis loop for $0.371 \leq h \leq 0.385$ and $\Omega = 0.5$ in Fig. 9. The ordinate intercept of each horizontal line in Fig. 9 is the number of prominent maxima of $\tilde{S}(k_0 \cos\theta, k_0 \cos\theta, \tau)$ as a function of θ for large τ, which is an order parameter distinguishing different spatial patterns. In contrast, a simple spatial average of the state variable s cannot distinguish between the stripe and polka-dot patterns, thus cannot serve as an order parameter.

§4. Concluding remarks

The scaling law (1·3) in the presence of external forcing is numerically confirmed for a stripe pattern with the scaling exponent $\alpha = 1/5$. We need a much larger system size to confirm the scaling law for a polka-dot pattern.

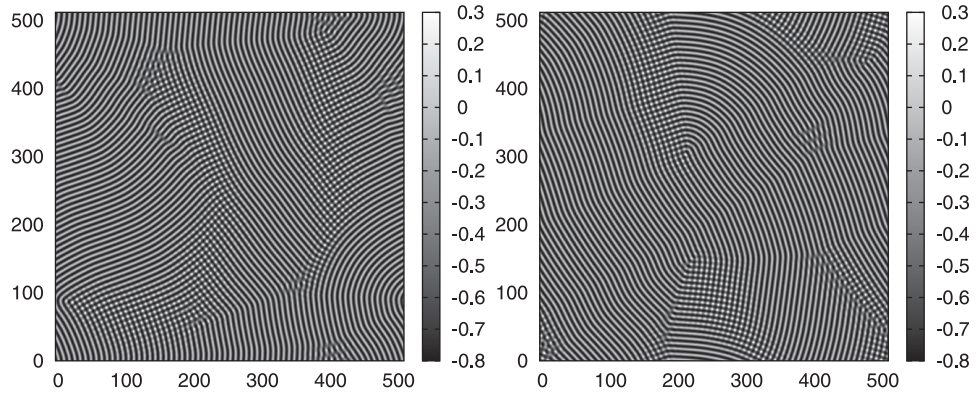

(a) (b)

Fig. 7. Snapshots of the asymptotic pattern of $s(\boldsymbol{r}, t)$ for $(h, \Omega) = (0.375, 0.5)$. The domains are painted in white for $s = 1$ and in black for $s = -1$. A gray scale is used for intermediate values of s between $s = -1$ and $s = 1$. The different sets of random initial conditions given in (a) and (b) yield different patchwork-like patterns consisting of a stripe part and a polka-dot part.

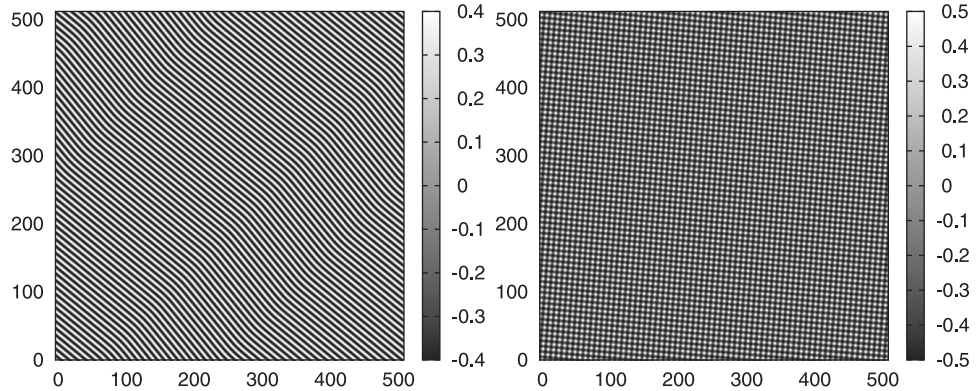

(a) Starting from stripe-pattern initial conditions

(b) Starting from polka-dot-pattern initial conditions

Fig. 8. Snapshots of the asymptotic pattern of $s(\boldsymbol{r}, t)$ for $(h, \Omega) = (0.375, 0.5)$ starting from two different special sets of initial conditions. First, an asymptotic numerical solution $s(\boldsymbol{r}, \tau)$ with large τ for $(h, \Omega) = (0.35, 0.5)$, yielding a global stripe pattern, is obtained. Then, this asymptotic solution is set as the initial conditions of $s(\boldsymbol{r}, 0)$ for $(h, \Omega) = (0.375, 0.5)$ in (a). In the same way, an asymptotic numerical solution $s(\boldsymbol{r}, \tau)$ with large τ for $(h, \Omega) = (0.41, 0.5)$, yielding a global polka-dot pattern, is chosen as the initial conditions of $s(\boldsymbol{r}, 0)$ for $(h, \Omega) = (0.375, 0.5)$ in (b). The domains are painted in white for $s = 1$ and in black for $s = -1$. A gray scale is used for intermediate values of s between $s = -1$ and $s = 1$.

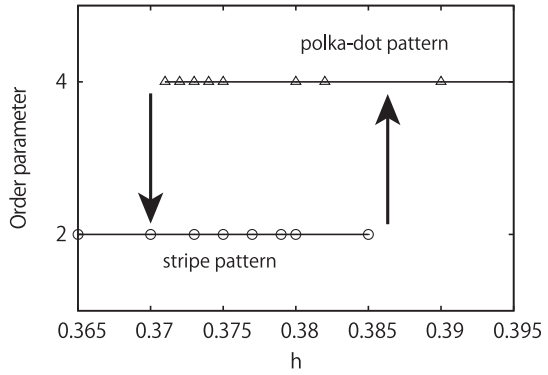

Fig. 9. Set of initial conditions $s(\boldsymbol{r}, 0)$ generated as an asymptotic numerical solution $s(\boldsymbol{r}, \tau)$ with large τ for a smaller value of h, yielding a global stripe pattern, leading to a global stripe pattern $s(\boldsymbol{r}, t)$ in the range $0.35 \leq h \leq 0.385$, which is plotted with the symbol ($\circ$) connected by the lower solid line. For $h > 0.385$, the above set of initial conditions is unstable and settles down to a global polka-dot pattern. In the same way, a set of initial conditions $s(\boldsymbol{r}, 0)$ generated as an asymptotic numerical solution $s(\boldsymbol{r}, \tau)$ with large τ for a larger value of h, yielding a global polka-dot pattern, leads to a global polka-dot pattern $s(\boldsymbol{r}, t)$ in the range $0.371 \leq h \leq 0.41$, which is plotted with the symbol ($\triangle$) connected by the upper solid line. For $h < 0.371$, the above set of initial conditions is unstable and settles down to a global stripe pattern. The ordinate intercept of each horizontal line is the number of prominent maxima of $\tilde{S}(k_0 \cos\theta, k_0 \cos\theta, \tau)$ as a function of θ for large τ. Sudden jumps between the stripe and polka-dot patterns are indicated by arrows. A hysteresis loop is observed.

It is known that the scaling exponents are different for the noiseless and noisy autonomous SH equations.[11),12)] In this paper, we first reported the pattern-dependent scaling behaviors in the case of periodically forced SH equation through the use of numerical simulations. Although we are still not able to give any theoretical argument to explain the pattern-dependent scaling behaviors, it will be important to show that the interactions between defects in the stripe pattern differ from those between defects in the polka-dot pattern.

Using the Ginzburg-Landau equation with a long-range interaction, Tsukamoto et al. studied the stability of a planar front with respect to transverse perturbations in bistable systems.[14)] It is well known that when a bistable system has competing short-range and long-range interactions, the front connecting two stable states can exhibit transverse instability. They focused on the effects of the nonlocal nature of the interaction, using long-range interactions with exponential decay (weak nonlocality) and power-law decay (strong nonlocality), and found that in the former case, the planar front can be stabilized by varying a parameter value, while in the latter case, the strong nonlocal nature of the interaction prevents stabilization of the front. As far as the final pattern shown in Fig. 1 is concerned, there is not much difference between the SH equation and the Ginzburg-Landau equation. This implies that the SH equation is a good phenomenological model of the magnetic domains of a garnet thin film in an oscillating magnetic field,[8),9)] whose experimental studies indeed motivated and inspired our investigation reported in this paper. It is a future problem to propose more realistic models that can be directly compared with the results of

these experiments.

Acknowledgements

We would like to thank Shoichi Kai and Yoshiki Hidaka for illuminating discussions. We also thank Takehiko Horita for careful reading of our manuscript and for useful comments.

References

1) M. C. Cross and P. C. Hohenberg, Rev. Mod. Phys. **65** (1993), 851.
2) P. Manneville, *Dissipative Structures and Weak Turbulence* (Academic Press, Boston, 1990).
3) G. Nicolis and I. Prigogine, *Self-Organization in Nonequilibrium Systems* (Wiley, New York, 1977).
4) J. Swift and P. C. Hohenberg, Phys. Rev. A **15** (1977), 319.
5) H. S. Greenside and M. C. Cross, Phys. Rev. A **31** (1985), 2492.
6) M. C. Cross, G. Tesauro and H. S. Greenside, Physica D **23** (1986), 12.
7) M' F. Hilali, S. Métens, P. Borckmans and G. Dewel, Phys. Rev. E **51** (1995), 2046.
8) G. S. Kandaurova, Phys. Usp. **45** (2002), 1051.
9) M. Mino, S. Miura, K. Dohi and H. Yamazaki, J. Magn. Magn. Mater. **226-230** (2001), 1530.
10) N. Tsukamoto, H. Fujisaka and K. Ouchi, Prog. Theor. Phys. Suppl. No. 161 (2006), 372.
11) K. R. Elder, J. Viñals and M. Grant, Phys. Rev. A **46** (1992), 7618.
12) K. R. Elder, J. Viñals and M. Grant, Phys. Rev. Lett. **68** (1992), 3024.
13) Q. Hou, S. Sasa and N. Goldenfeld, Physica A **239** (1997), 219.
14) N. Tsukamoto, H. Fujisaka and K. Ouchi, Prog. Theor. Phys. **119** (2008), 1.